^{18}F-FLT PET/CT in the Evaluation of Pheochromocytomas and Paragangliomas: A Pilot Study

Elise M. Blanchet*[1], David Taieb*[2], Corina Millo[3], Victoria Martucci[1], Clara C. Chen[4], Maria Merino[5], Peter Herscovitch[3], and Karel Pacak[1]

[1]*Program in Reproductive and Adult Endocrinology, Eunice Kennedy Shriver National Institute of Child Health and Human Development (NICHD), National Institutes of Health, Bethesda, Maryland;* [2]*La Timone University Hospital, European Center for Research in Medical Imaging, Aix-Marseille University, Marseille, France;* [3]*Positron Emission Tomography Department, Warren Grant Magnuson Clinical Center, National Institutes of Health, Bethesda, Maryland;* [4]*Nuclear Medicine Department, Warren Grant Magnuson Clinical Center, National Institutes of Health, Bethesda, Maryland; and* [5]*Laboratory of Pathology, National Cancer Institute, National Institutes of Health, Bethesda, Maryland*

^{18}F-FDG PET/CT has been proven to be a highly sensitive method for pheochromocytomas/paragangliomas (PHEOs/PGLs) associated with succinate dehydrogenase (SDH) mutations. This finding has been attributed to altered tumor cell metabolism resulting from these mutations and does not provide additional prognostic information to genotype. Therefore, identification of new biomarkers for aggressiveness is needed. A high Ki-67 index was proposed to be an additional prognostic factor. This pilot study aimed to evaluate 3′-deoxy-3′-^{18}F-fluorothymidine (^{18}F-FLT) PET/CT, a PET proliferation tracer, as a potential imaging agent in a series of 12 PHEO/PGL patients with different genetic backgrounds, to compare ^{18}F-FLT uptake with ^{18}F-FDG PET/CT, and to evaluate classic factors of aggressiveness. **Methods:** Twelve patients (7 metastatic and 5 nonmetastatic) were prospectively evaluated with ^{18}F-FDG and ^{18}F-FLT and followed for at least 2 y after the initial imaging work-up. Uptake was assessed at a lesion level, visually and quantitatively by maximum standardized uptake values (SUV_{max}) for both tracers. ^{18}F-FLT uptake was compared with risk factors known to be linked with a poor prognosis in PGLs (*SDHB*-mutated status, lesion size, dopaminergic phenotype) and with ^{18}F-FDG uptake. **Results:** In 12 patients, 77 lesions were assessed. All lesions had low ^{18}F-FLT uptake (median SUV_{max}, 2.25; range, 0.7–4.5). There was no apparent superiority of ^{18}F-FLT uptake in progressive lesions, and most of the lesions showed a mismatch, with high ^{18}F-FDG uptake (median SUV_{max}, 10.8; range, 1.1–79.0) contrasting with low ^{18}F-FLT uptake. **Conclusion:** This study suggests that PHEOs/PGLs—even those that progress—do not exhibit intense ^{18}F-FLT uptake. It provides the first in vivo demonstration that proliferation may not be a major determinant of ^{18}F-FDG uptake in these tumors. These findings provide new insight into the biologic behavior of PGL and suggest that antiproliferative agents may be suboptimal for treatment of these tumors.

Key Words: pheochromocytoma and paraganglioma; ^{18}F-fluorothymidine; ^{18}F-fluorodeoxyglucose; positron emission tomography; proliferation; glycolysis

J Nucl Med 2015; 56:1849–1854
DOI: 10.2967/jnumed.115.159061

Pheochromocytomas (PHEOs) and extraadrenal paragangliomas (PGLs) are neural crest cell–derived tumors associated with either the sympathetic (thoracoabdominal PGLs) or the parasympathetic (mainly head and neck PGLs) nervous systems.

Approximately 40% of PHEOs and PGLs carry a germline mutation in 1 of at least 18 genes (*1*). These mutations are associated with transcriptome changes that are currently subdivided into 2 main clusters. Cluster 1 is enriched with genes (i.e., succinate dehydrogenase complex, subunits A-D [SDHx]) that are associated with the hypoxic response (mainly hypoxia-inducible factor [HIF]-2α), and cluster 2 contains tumors mutated for genes that activate kinase signaling and protein translation (i.e., RET protooncogene-MEN2) (*2*).

Overall, the malignancy risk for PHEOs/PGLs has been estimated to be 10%, with an increased risk in sympathetic PGLs belonging to the cluster 1 subgroup.

At the present time, there are no reliable cytologic, histologic, immunohistochemical, molecular, or imaging criteria for determining malignancy (*3*). The diagnosis of malignancy remains strictly based on the finding of metastases where paraganglial cells are not usually present, such as the lymph nodes, lung, bone, or liver. To this end, anatomic and functional imaging play a central role in ruling out metastases but are still limited in that they cannot provide further information about the potential behavior (e.g., malignant potential, proliferation rate, degree of apoptosis, and hypoxia) of these tumors that is closely linked to their genotype, biochemical properties, and localization.

Beyond *SDHB* mutation status, classic indicators of poor prognosis include a tumor size greater than 5 cm, tumor location (extraadrenal), age younger than 30 y at first presentation, and metastatic disease (*4–6*). Recently, some new studies have proposed the prediction of metastatic potential or tumor aggressiveness using characteristics such as dopaminergic phenotype (i.e., detection of dopamine or its metabolite methoxytyramine) (*7,8*), the presence of tumor necrosis, high Ki-67 index or mitotic count (*9*), overexpression of HIF-α and its target

Received Apr. 9, 2015; revision accepted Jun. 23, 2015.
For correspondence or reprints contact: Karel Pacak, Section on Medical Neuroendocrinology, Program in Reproductive and Adult Endocrinology, NICHD, NIH, Building 10, CRC, 1-East, Rm. 1-3140, 10 Center Dr., MSC-1109, Bethesda, MD 20892-1109.
E-mail: karel@mail.nih.gov
*Contributed equally to this work.
Published online Sep. 10, 2015.

genes in tumors (*10,11*), or extremely high messenger RNA copy numbers of a variant of carboxypeptidase E in tumors (*12*). Thus, the identification of in vivo biomarkers of aggressiveness would be of particular interest in the assessment of these tumors.

Interestingly, PHEOs/PGLs belonging to the cluster 1 exhibit increased ^{18}F-FDG uptake on PET/CT, compared with cluster 2 tumors (*13*). ^{18}F-FDG PET/CT has been proven to provide prognostic information in several endocrine cancers such as thyroid carcinomas of follicular origin (*14*), medullary thyroid carcinoma (*15*), and gastroenteropancreatic neuroendocrine tumors (*16*). In these tumors, acquisition of the ^{18}F-FDG metabolic pattern is progressive during the dedifferentiation process. In contrast, ^{18}F-FDG PET/CT avidity was found to be mainly dependent on the presence of a pseudohypoxic phenotype (activation of the HIF-signaling pathway despite normal oxygen supply) in PHEOs/PGLs, a finding that is in large part dependent on the genetic background (cluster 1 genes) (*2,13,17,18*). Therefore, the ^{18}F-FDG PET/CT avidness does not provide prognostic information in PHEOs/PGLs, and SDHx tumors may have an indolent course, even with highly elevated uptake values of ^{18}F-FDG.

3′-deoxy-3′-^{18}F-fluorothymidine (^{18}F-FLT) has been proposed as a PET proliferation tracer even though it is not incorporated into DNA because of phosphorylation by cytosolic thymidine kinase-1. The assumption is that the concentration of ^{18}F-FLT nucleotides in cells is proportional to thymidine kinase-1 activity and, therefore, to cellular proliferation. The role of ^{18}F-FLT in oncology is still debated, but several studies have shown promising results for tumor grading and in the evaluation of treatment response (*19*).

The aims of the present study were to evaluate ^{18}F-FLT PET/CT in a series of 12 PHEO/PGL patients with varying genetic backgrounds and to evaluate the relationships between ^{18}F-FLT uptake and classic factors of aggressiveness (e.g., presence of *SDHB* mutation, age $\leq$ 30 y at diagnosis, metastatic disease, large lesions [>5 cm], and elevated dopamine secretion). ^{18}F-FDG PET/CT was also performed with head-to-head comparison between ^{18}F-FDG and ^{18}F-FLT lesion uptake in order to better understand the relationship between glycolysis and cell proliferation in these tumors.

MATERIALS AND METHODS

Patients

Twelve nonconsecutive adult patients (10 men and 2 women; median age, 43 y; age range, 27–70 y) with PGLs (as defined by the reference standard) were prospectively included between January and July 2012 (and followed up over the course of at least 2 y). All patients were studied at the National Institutes of Health. The study protocol (00-CH-0093) was approved by the Institutional Review Board of the Eunice Kennedy Shriver National Institute of Child Health and Human Development, National Institutes of Health, and all subjects provided written informed consent. The inclusion criterion was to have at least 1 PGL (as defined by the reference standard) at the time of the study. Exclusion criteria included age younger than 18 y, pregnancy, or recent (<2 mo) systemic treatment.

Reference Standard to Define PGL

PGL lesions were confirmed histologically when surgery was performed on patients with nonmetastatic disease (patients 1, 2, 5, 8, and 9). When surgery was not indicated because of the presence of metastases (patients 3, 4, 6, 7, 10, 11, and 12), lesions were characterized as PGL-related (either primary or metastatic) based on their positivity (characteristic appearance) on conventional imaging—either contrast-enhanced CT or contrast-enhanced MR imaging—that corresponded with positivity on either 6-^{18}F-fluoro-3,4-dihydroxyphenylalanine (^{18}F-FDOPA) or 6-^{18}F-fluorodopamine (^{18}F-FDA) PET/CT (*13,20,21*); these findings were further supported by positive PGL-specific biochemistry and genetic testing results.

The following data were collected: metastatic status (defined by the presence of tumor cells at nonneural crest–derived sites), genetic testing, adrenal versus extraadrenal location, tumor size (patient carrying at least 1 tumor diameter > 5 cm, which is the optimal cutoff from Eisenhofer's analysis (*8*)), dopaminergic phenotype (i.e., presence of dopamine or its metabolite methoxytyramine in urine or plasma (*8*)), and age at diagnosis. Patients were followed (clinically, biochemically, and with imaging) for at least 2 y after their initial imaging.

Imaging Protocol for ^{18}F-FDG and ^{18}F-FLT PET/CT Scans

All patients underwent ^{18}F-FDG and ^{18}F-FLT PET/CT scanning. ^{18}F-FLT was provided by Cardinal Health. A fixed ^{18}F-FLT dose of 195 MBq was injected. For ^{18}F-FDG PET scanning, patients fasted for at least 4 h before intravenous injection of ^{18}F-FDG (5 MBq/kg; median total injected dose, 390 MBq; range, 340–590 MBq), and blood glucose levels were measured just before injection to ensure a value below 200 mg/dL. For both radiopharmaceuticals, PET/CT acquisitions were performed on a Biograph-128 mCT PET/CT scanner (Siemens Medical Solutions). For both studies, PET data acquisition started at 60 min after injection. Emission images were obtained in 3-dimensional mode, with 3-min per bed position and 5-min per bed position rates for ^{18}F-FDG and ^{18}F-FLT, respectively. The acquisitions were done from the thighs to the head. Coregistered CT studies for attenuation correction and anatomic coregistration were performed with the following imaging parameters: 120 kV, 115 mA, and a 1.5-mm section thickness. Coregistered images were displayed on a workstation (DeltaViewer; MedImage), with 3-dimensional fused navigation along the axial, coronal, and sagittal planes and maximum-intensity-projection rendering.

^{18}F-FLT and ^{18}F-FDG PET/CT scans were obtained within 1 mo of each other in all but 1 case, with ^{18}F-FLT obtained first in 2 patients (patients 2 and 6) and ^{18}F-FDG performed first in the 10 other patients. For patient 10, the ^{18}F-FLT scan was acquired 4 mo after the ^{18}F-FDG scan.

^{18}F-FDG and ^{18}F-FLT PET Image Analysis

On ^{18}F-FLT and ^{18}F-FDG PET/CT images, uptake was assessed for each lesion (determined on the basis of CT) visually (intensity of uptake in comparison to the surrounding background and to reference organs) and quantitatively. Uptake values were classified according to their location: soft tissue for lesions located in the head and neck area, mediastinum, lung, liver, extrahepatic abdomen and pelvis, and bone. In the case of multiple lesions, a cutoff of 5 lesions per area was fixed.

For quantitative assessment, body weight maximum standardized uptake values (SUV_{max}) were calculated using the following formula: standardized uptake value (SUV) equals decay-corrected tracer tissue concentration (in Bq/g) injected dose (in Bq) normalized by the patient's body weight (in g). In both ^{18}F-FLT and ^{18}F-FDG PET, volumes of interest were determined manually over the lesions using coregistered CT. Some small lesions that could not be separated easily from surrounding physiologic uptake (such as in the cases of small liver and bone lesions) were considered nonmeasurable. The largest diameter of each lesion was measured.

Physiologic ^{18}F-FLT uptake was also quantified by SUV_{max} in the following normal organs: bone marrow (in the L4 vertebral body) and lymphatic tissue (including nonspecific inflammatory lymph nodes, tonsils, and thymic remnants) for use as intrapatient positive controls, and muscle (right paravertebral muscle at the level of L4) for use as an intrapatient nonproliferative negative control. Indeed hematopoietic cells in bone marrow and (to a lesser extent) lymphatic tissue were highly ^{18}F-FLT–positive, as expected for active proliferative tissues (*22,23*). Liver uptake was also measured.

TABLE 1
Patient Clinical Characteristics

Patient no.	Age (y), sex	Germline mutation	Age at initial diagnosis	Status at the time of ^{18}F-FLT and ^{18}F-FDG PET	Size of largest lesion at time of ^{18}F-FLT/^{18}F-FDG	Dopamine secretion	Reason for evaluation at time of ^{18}F-FLT and ^{18}F-FDG PET	Previous systemic treatments (delay between end of last treatment and PET scan)	2-y follow-up (progression or death from PGL)
1	43, M	Sporadic	43	Primary	3.8 cm	Negative	Suspected primary	None	No
2	43, M	SDHD	43	Primary	4.8 cm	Negative	Suspected primary	None	No
3	43, M	SDHD	41	Primary	4.7 cm	Negative	Restaging	None	No
4	48, F	MEN2	35	Metastatic	12 cm	Negative	Restaging	^{131}I-metaiodobenzylguanidine (>2 y)	No
5	47, M	Sporadic	30	Metastatic	Unknown	Negative	Suspected recurrence	None	No
6	70, M	Sporadic	67	Metastatic	24 cm	Negative	Suspected recurrence	None	No
7	50, F	Sporadic	43	Metastatic	8 cm	Negative	Restaging	^{131}I-metaiodobenzylguanidine (8 mo), sandostatin therapy (on)	No
8	30, M	SDHB	30	Primary	2.5 cm	Negative	Initial staging	None	No
9	27, M	SDHB	27	Primary	3 cm	Negative	Initial staging	None	No
10	35, M	SDHB	19	Metastatic	8 cm	Positive	Restaging	None	Yes
11	35, M	SDHB	25	Metastatic	7 cm	Positive	Restaging	CVD (>2 y), ^{131}I-metaiodobenzylguanidine (4 mo)	Yes
12	47, M	SDHB	41	Metastatic	3 cm	Negative	Restaging	CVD (2 mo)	Yes

CVD = cyclophosphamide, vincristine, and dacarbazine.

Histopathologic Analyses and Immunohistochemical Staining

Histopathologic analyses and immunohistochemical staining were performed in 5 patients with nonmetastatic disease in whom tumor tissue was collected prospectively after an ^{18}F-FLT PET scan. Cell and tissue morphology and immunohistochemical staining (chromogranin and synaptophysin) confirmed the diagnosis of PGL, and then Ki-67 levels were assessed. No patient with metastatic disease underwent surgery for ethical reasons: PGL diagnosis could noninvasively be confirmed using imaging, biochemistry, and medical history, and PGL biopsy can lead to severe adverse events related to catecholamine release.

Genetic Testing

Genetic testing included gene sequencing of *SDHB, SDHD, RET,* and *VHL* as well as assessment of large gene rearrangements of *SDHB* and *SDHD*. When all these were negative, patients were qualified apparently sporadic. Patients were not tested for mutations in the recently described genes *SDHA, SDHAF2,* and *TMEM127*.

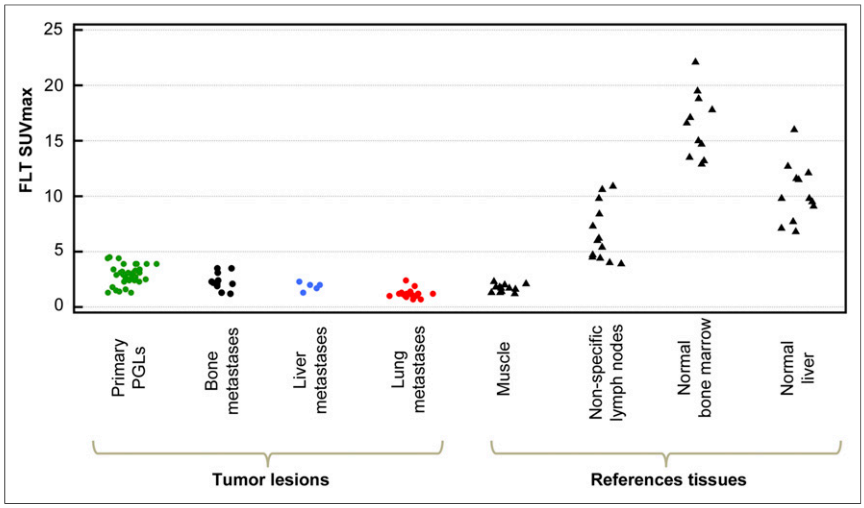

FIGURE 1. ^{18}F-FLT SUV_{max} in lesions and reference organs. PGLs: includes all PGLs (primary tumors only) from patients with metastatic and nonmetastatic disease. Median number of primary PGLs assessed per patient was 3 (range, 1–9). In patients 7, 11, and 12, bone marrow ^{18}F-FLT SUV_{max} was not measured because of disseminated metastatic bone disease.

Statistical Analysis

Descriptive quantitative data were expressed as either a median or given a range. The correlation between ^{18}F-FLT SUV and ^{18}F-FDG SUV was assessed using the Spearman rank correlation coefficient. A P value of less than 0.05 was considered statistically significant.

RESULTS

Patients, Tumors, and Clinical Outcomes

Twelve patients with PHEO/PGL were studied (5 SDHB, 2 SDHD, 1 MEN2, and 4 sporadic). Seven patients were M1, and 5 were M0. Four patients were at the initial stages of PGL disease, 2 were evaluated

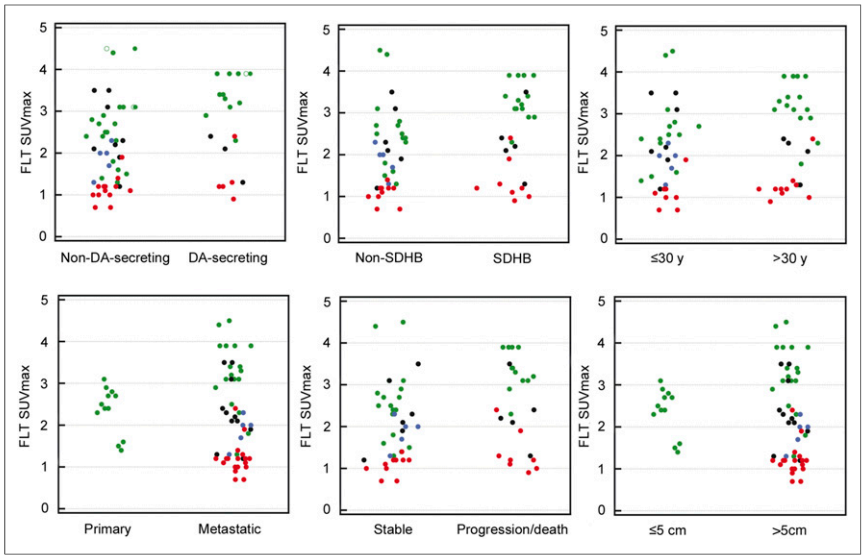

FIGURE 2. Lesion ^{18}F-FLT SUV_{max} compared with criteria of poor prognosis. Green, black, blue, and red refer to primary PGLs, bone metastases, liver metastases, and lung metastases, respectively.

for recurrence, and 6 for disease progression. One patient had an adrenal PGL, and 11 patients had extraadrenal PGLs. Seven patients had a history of a voluminous (>5 cm) primary PHEO/PGL lesion. Seven patients had previously received antioncologic therapy (^{131}I-metaiodobenzylguanidine in 3 cases; cyclophosphamide, vincristine, and dacarbazine [CVD] chemotherapy in 2 cases; external-beam radiation therapy in 2 cases). Patient characteristics are detailed in Table 1.

After ^{18}F-FLT PET scanning, 3 patients (patients 10–12) had progressive disease (all associated with the *SDHB*-mutated genotype, 2/3 with the dopaminergic phenotype). The remaining 9 patients had stable or slowly progressing disease (Table 1).

Seventy-seven lesions were assessed. Of these, 14 lesions were in patients with only primary lesions, and 63 lesions were in patients carrying metastatic lesions. Metastatic sites included soft tissue (lymph nodes) (19), bones (16), liver (10), and lungs (18).

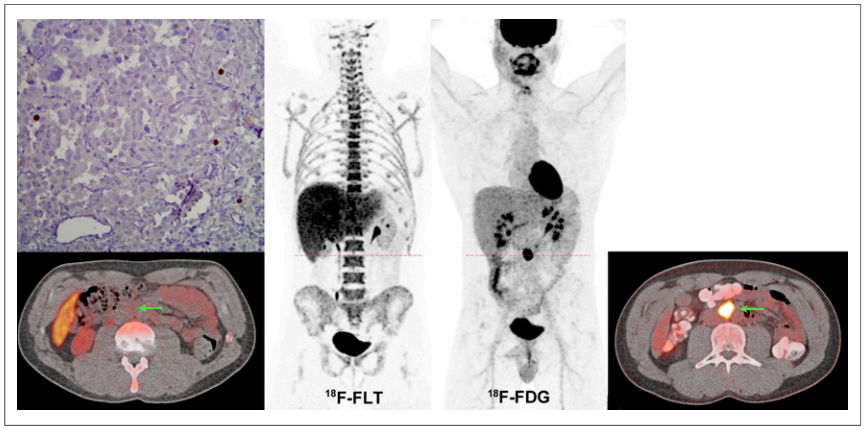

FIGURE 3. Single retroperitoneal primary PGL in *SDHB* patient (patient 3). ^{18}F-FDG (maximum-intensity-projection [MIP] image and axial CT–fused image at level of PGL lesion) shows particularly high uptake (^{18}F-FDG SUV_{max}, 59.8). This lesion corresponded to a 2.6-cm abdominal extraadrenal mass (arrows). ^{18}F-FLT (MIP image and axial CT–fused image at level of PGL lesion) shows low uptake (^{18}F-FLT SUV_{max}, 2.5). Low Ki-67 staining is demonstrated.

^{18}F-FLT Uptake in PGL Lesions

Of the 77 lesions, 64 were measurable using SUV_{max}. Thirteen small lesions were nonmeasurable because of surrounding tissue activity: 2 primary PGLs, 6 bone lesions, and 5 liver lesions.

The average tumor ^{18}F-FLT SUV_{max} was 2.25 (0.7–4.5). ^{18}F-FLT uptake was also observed in normal bone marrow and liver in all cases. In 4 patients (patients 2, 3, 5, and 9), ^{18}F-FLT uptake was noted in 13 lymph nodes/lymphatic tissue–related sites (including tonsils and thymic remnants) thought unrelated to the presence of PHEO/PGL (based on negativity of ^{18}F-FDOPA and ^{18}F-FDA studies). Figure 1 displays the ^{18}F-FLT SUV_{max} in lesions and reference organs.

^{18}F-FLT in PGL Compared with Clinical Criteria of Poor Prognosis (Per-Patient Analysis)

No significant differences in tumor ^{18}F-FLT SUV_{max} were observed between patients segregated by the presence or absence of poor prognostic factors, including *SDHB* versus non-*SDHB* (2.9 [0.9–3.9] vs. 1.9 [0.7–4.5]), age 30 y or younger versus older than 30 y at diagnosis (2.35 [0.9–3.9] vs. 2.05 [0.7–4.5]), metastatic versus nonmetastatic disease (2.05 [0.7–4.5] vs. 2.45 [1.4–3.1]), presence or absence of large (>5 cm) lesions (3.25 [1.3–4.5] vs. 2.45 [1.4–3.1], and elevated versus normal dopamine secretion (median, 2.9 [range, 0.9–3.9] vs. 2.0 [0.7–4.5]). There was also no significant difference in uptake of lesions in patients who had progressive versus stable disease during follow-up (2.4 [0.9–3.9] vs. 2.0 [0.7–4.5]). Figure 2 displays the average ^{18}F-FLT SUV_{max} in lesions according to these prognostic factors and follow-up.

Comparison of ^{18}F-FLT Uptake in PGL with ^{18}F-FDG Uptake

On visual analysis, most lesions (66/77) showed a discrepancy between ^{18}F-FLT and ^{18}F-FDG uptake, with high ^{18}F-FDG uptake contrasting with low or absent ^{18}F-FLT uptake. Figure 3 shows the example of an *SDHB* patient with a primary abdominal PGL, and Figure 4 is an example of an *SDHB* patient with widespread metastatic disease.

Overall, the average ^{18}F-FDG SUV_{max} of the 77 lesions was 10.8 (1.1–79.0), compared with an average SUV_{max} of 2.25 (0.7–4.5) for ^{18}F-FLT. Correlation analysis demonstrated a weak positive correlation between ^{18}F-FLT and ^{18}F-FDG uptake expressed by SUV_{max} (Spearman ρ, 0.62; $P < 0.05$—Fig. 5 shows the scatterplot). Similarly, correlation analyses conducted on subgroups (*SDHB*-related tumors, non-*SDHB*–related tumors) demonstrated a weak positive correlation between the ^{18}F-FLT and ^{18}F-FDG SUV_{max} (Spearman ρ, 0.40, and $P = 0.11$ for SDHB; and Spearman ρ, 0.59, and $P < 0.05$ for non-SDHB).

Ki-67 Immunostaining

In vitro proliferative activity as assessed by Ki-67 index was low (<5%) in all surgically

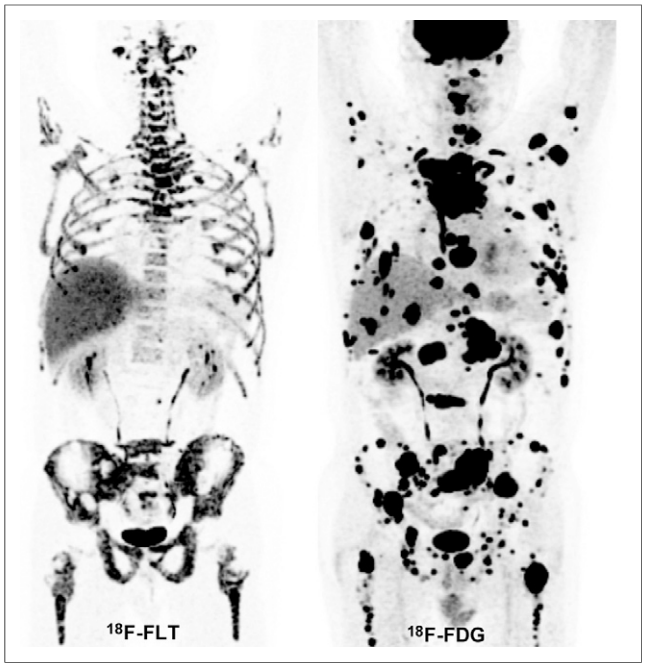

FIGURE 4. Disseminated metastatic disease (soft tissue, bone, liver, and lung lesions) in *SDHB* patient. ^{18}F-FDG (maximum-intensity-projection [MIP] image) shows high tumor burden with high ^{18}F-FDG uptake in most of the lesions. ^{18}F-FLT (MIP image) shows low ^{18}F-FLT uptake. Bone lesions (notably in both femoral heads and bilateral iliac bones) appear to have relatively low ^{18}F-FLT uptake compared with surrounding background uptake in marrow.

resected lesions (patients 1, 2, 5, 8, and 9). The average ^{18}F-FLT and ^{18}F-FDG SUV_{max} was, respectively, 2.8 and 6.5 in patient 1, 2.7 and 14.5 in patient 2, 3.1 and 10.4 in patient 5, 2.9 and 53.2 in patient 8, and 3.1 and 46.9 in patient 9.

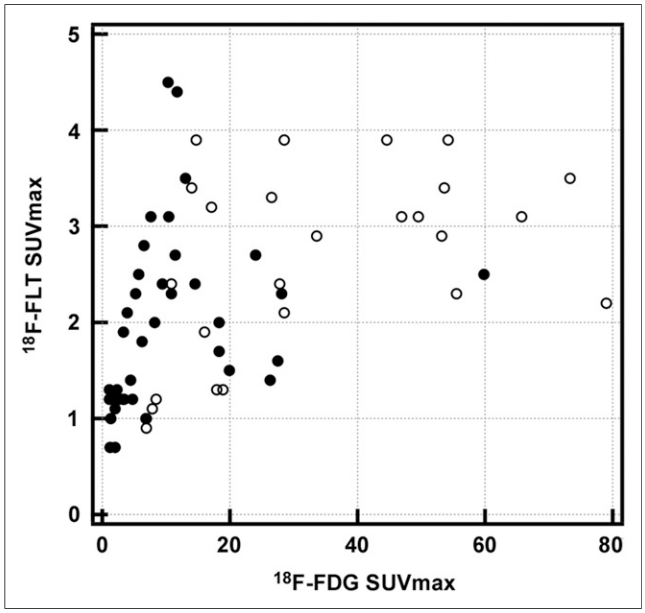

FIGURE 5. Scatterplot displaying tumor ^{18}F-FLT SUV_{max} in relation to their ^{18}F-FDG SUV_{max}. ● = lesions from non-*SDHB* patients; ○ = lesions from non-*SDHB* patients. Correlation analysis demonstrated positive correlation between ^{18}F-FLT and ^{18}F-FDG uptake (Spearman ρ, 0.62; $P < 0.05$).

DISCUSSION

This study shows that PHEOs/PGLs did not exhibit intense ^{18}F-FLT uptake in our 12 patients, even those who progressed rapidly or exhibited high ^{18}F-FDG uptake. It also provides the first, to our knowledge, in vivo demonstration that proliferation is probably not a major determinant of ^{18}F-FDG uptake in these lesions.

These findings differ from highly proliferative cancers (i.e., lymphoma, lung cancer) that exhibit high ^{8}F-FLT tumor uptake values (*19*). However, the low ^{18}F-FLT uptake found in PGL is concordant with findings observed in well-differentiated gastroenteropancreatic tumors. In 1 study, none of the tumors (primary lesions or metastases) were positive on ^{18}F-FLT PET/CT whereas ^{18}F-FDG PET/CT was positive in 7 of 10 cases (*24*). ^{18}F-FLT PET/CT was also found to be less sensitive than ^{18}F-FDG PET/CT in the diagnosis of residual lymph node and distant metastases from differentiated thyroid carcinoma (*25*). Primary papillary thyroid carcinomas detected by ^{18}F-FDG PET/CT were also found to have low ^{18}F-FLT uptake, a finding that was attributed to a low proliferation activity (*26*).

To our best knowledge, ^{18}F-FLT PET/CT has not been evaluated in other endocrine malignancies. Our results are consistent with the low proportion of PHEOs/PGLs with high Ki-67 indices (*27–29*) and provide in vivo evidence of low proliferation rates of PHEO/PGL metastases. These results are also consistent with preclinical models showing that PHEO/PGL tumor cells were mostly at the resting state of the cell cycle (the so-called G0/G1 transition) (*30*). ^{18}F-FLT SUV_{max} was also not associated with the presence of certain criteria for poor prognosis. Resistance, invasiveness, and establishment of micrometastases of these pseudohypoxic cells might rather contribute to tumor aggressiveness than proliferation and the final outcome of a patient's disease.

Our study also provides the first in vivo demonstration that proliferation is not a major determinant of ^{18}F-FDG uptake in these tumors, including *SDH*x-related tumors, which often exhibit highly elevated uptake values (*13,17*). This finding has been attributed to activation of the HIF-α pathway despite normal or even high oxygen supply (also called the pseudohypoxic phenotype). On the basis of our recent metabolomic study, it has been proposed that glucose might be directly or indirectly involved in the metabolism of myoinositol/ascorbate, glutamine/glutamate, methionine/taurine, and catecholamines (*31*).

The main limitation of the study was related to the small number of patients evaluated by ^{18}F-FLT PET/CT with widely heterogeneous characteristics. Some patients had also been treated in the past with therapeutic approaches that may have modified ^{18}F-FLT uptake (Table 1). However, all of these patients were refractory to these therapies.

There is currently no effective treatment for metastatic PHEOs and PGLs. Treatment experience with cytotoxic chemotherapy using different drugs and regimens is limited and associated with high-grade toxicities (*32*). The most effective chemotherapy regimen appears to be the CVD scheme. A deficiency in current chemotherapy-using drugs that target dividing tumor cells has been attributed to the slow growing pattern of most PHEOs and PGLs, even metastatic ones (*33*). Preclinical studies have also stated that these drugs might be effective if we push experimental cells into other phases (*30*). Our in vivo findings also suggest that the development of antiproliferative agents may not be effective in the treatment of these tumors because primary and metastatic lesions exhibit low ^{18}F-FLT avidity.

CONCLUSION

In this limited pilot study, ^{18}F-FLT uptake was relatively low in PGL tumors, even metastatic and rapidly growing ones; therefore, ^{18}F-FLT PET/CT should not be used for PGL grading and in the evaluation of their treatment responses. From a pathophysiologic standpoint, this study also provides in vivo evidence of a low proliferative rate despite high ^{18}F-FDG uptake present in the same lesions. Nevertheless, the conclusions of the present study should be tested on a larger population of patients, including all currently known hereditary PGLs as well as recurrent and locally aggressive ones.

DISCLOSURE

The costs of publication of this article were defrayed in part by the payment of page charges. Therefore, and solely to indicate this fact, this article is hereby marked "advertisement" in accordance with 18 USC section 1734. This work was supported by the Intramural Research Program of the Eunice Kennedy Shriver National Institute of Child Health and Human Development, National Institutes of Health. No other potential conflict of interest relevant to this article was reported.

REFERENCES

1. Martucci VL, Pacak K. Pheochromocytoma and paraganglioma: diagnosis, genetics, management, and treatment. *Curr Probl Cancer.* 2014;38:7–41.
2. van Berkel A, Rao JU, Kusters B, et al. Correlation between in vivo ^{18}F-FDG PET and immunohistochemical markers of glucose uptake and metabolism in pheochromocytoma and paraganglioma. *J Nucl Med.* 2014;55:1253–1259.
3. Gimm O, DeMicco C, Perren A, Giammarile F, Walz MK, Brunaud L. Malignant pheochromocytomas and paragangliomas: a diagnostic challenge. *Langenbecks Arch Surg.* 2012;397:155–177.
4. Amar L, Baudin E, Burnichon N, et al. Succinate dehydrogenase B gene mutations predict survival in patients with malignant pheochromocytomas or paragangliomas. *J Clin Endocrinol Metab.* 2007;92:3822–3828.
5. Ayala-Ramirez M, Feng L, Johnson MM, et al. Clinical risk factors for malignancy and overall survival in patients with pheochromocytomas and sympathetic paragangliomas: primary tumor size and primary tumor location as prognostic indicators. *J Clin Endocrinol Metab.* 2011;96:717–725.
6. Schovanek J, Martucci V, Wesley R, et al. The size of the primary tumor and age at initial diagnosis are independent predictors of the metastatic behavior and survival of patients with SDHB-related pheochromocytoma and paraganglioma: a retrospective cohort study. *BMC Cancer.* 2014;14:523.
7. Peitzsch M, Prejbisz A, Kroiss M, et al. Analysis of plasma 3-methoxytyramine, normetanephrine and metanephrine by ultraperformance liquid chromatography-tandem mass spectrometry: utility for diagnosis of dopamine-producing metastatic phaeochromocytoma. *Ann Clin Biochem.* 2013;50:147–155.
8. Eisenhofer G, Lenders JW, Siegert G, et al. Plasma methoxytyramine: a novel biomarker of metastatic pheochromocytoma and paraganglioma in relation to established risk factors of tumour size, location and SDHB mutation status. *Eur J Cancer.* 2012;48:1739–1749.
9. de Wailly P, Oragano L, Rade F, et al. Malignant pheochromocytoma: new malignancy criteria. *Langenbecks Arch Surg.* 2012;397:239–246.
10. Pinato DJ, Ramachandran R, Toussi ST, et al. Immunohistochemical markers of the hypoxic response can identify malignancy in phaeochromocytomas and paragangliomas and optimize the detection of tumours with VHL germline mutations. *Br J Cancer.* 2013;108:429–437.
11. Span PN, Rao JU, Oude Ophuis B, et al. Overexpression of the natural antisense hypoxia-inducible factor-1α transcript is associated with malignant phaeochromocytoma/paraganglioma. *Endocr Relat Cancer.* 2011;18:323–331.
12. Murthy SR, Pacak K, Loh YP. Carboxypeptidase E: elevated expression correlated with tumor growth and metastasis in pheochromocytomas and other cancers. *Cell Mol Neurobiol.* 2010;30:1377–1381.
13. Timmers HJ, Chen CC, Carrasquillo JA, et al. Staging and functional characterization of pheochromocytoma and paraganglioma by ^{18}F-fluorodeoxyglucose (^{18}F-FDG) positron emission tomography. *J Natl Cancer Inst.* 2012;104:700–708.
14. Robbins RJ, Wan Q, Grewal RK, et al. Real-time prognosis for metastatic thyroid carcinoma based on 2-[^{18}F]fluoro-2-deoxy-d-glucose-positron emission tomography scanning. *J Clin Endocrinol Metab.* 2006;91:498–505.
15. Adams S, Baum R, Rink T, Schumm-Drager PM, Usadel KH, Hor G. Limited value of fluorine-18 fluorodeoxyglucose positron emission tomography for the imaging of neuroendocrine tumours. *Eur J Nucl Med.* 1998;25:79–83.
16. Garin E, Le Jeune F, Devillers A, et al. Predictive value of ^{18}F-FDG PET and somatostatin receptor scintigraphy in patients with metastatic endocrine tumors. *J Nucl Med.* 2009;50:858–864.
17. Taieb D, Sebag F, Barlier A, et al. ^{18}F-FDG avidity of pheochromocytomas and paragangliomas: a new molecular imaging signature? *J Nucl Med.* 2009;50:711–717.
18. Taïeb D, Timmers HJ, Shulkin BL, Pacak K. Renaissance of ^{18}F-FDG positron emission tomography in the imaging of pheochromocytoma/paraganglioma. *J Clin Endocrinol Metab.* 2014;99:2337–2339.
19. Tehrani OS, Shields AF. PET imaging of proliferation with pyrimidines. *J Nucl Med.* 2013;54:903–912.
20. Gabriel S, Blanchet EM, Sebag F, et al. Functional characterization of nonmetastatic paraganglioma and pheochromocytoma by ^{18}F-FDOPA PET: focus on missed lesions. *Clin Endocrinol (Oxf).* 2013;79:170–177.
21. Timmers HJ, Chen CC, Carrasquillo JA, et al. Comparison of ^{18}F-fluoro-L-DOPA, ^{18}F-fluoro-deoxyglucose, and ^{18}F-fluorodopamine PET and ^{123}I-MIBG scintigraphy in the localization of pheochromocytoma and paraganglioma. *J Clin Endocrinol Metab.* 2009;94:4757–4767.
22. Agool A, Schot BW, Jager PL, Vellenga E. ^{18}F-FLT PET in hematologic disorders: a novel technique to analyze the bone marrow compartment. *J Nucl Med.* 2006;47:1592–1598.
23. Troost EG, Vogel WV, Merkx MA, et al. ^{18}F-FLT PET does not discriminate between reactive and metastatic lymph nodes in primary head and neck cancer patients. *J Nucl Med.* 2007;48:726–735.
24. Giammarile F, Billotey C, Lombard-Bohas C, et al. ^{18}F-FLT and ^{18}F-FDG positron emission tomography for the imaging of advanced well-differentiated gastro-entero-pancreatic endocrine tumours. *Nucl Med Commun.* 2011;32:91–97.
25. Nakajo M, Jinguji M, Tani A, et al. Diagnosis of metastases from postoperative differentiated thyroid cancer: comparison between FDG and FLT PET/CT studies. *Radiology.* 2013;267:891–901.
26. Nakajo M, Kajiya Y, Jinguji M, et al. High FDG and low FLT uptake in a thyroid papillary carcinoma incidentally discovered by FDG PET/CT. *Clin Nucl Med.* 2012;37:607–608.
27. Strong VE, Kennedy T, Al-Ahmadie H, et al. Prognostic indicators of malignancy in adrenal pheochromocytomas: clinical, histopathologic, and cell cycle/apoptosis gene expression analysis. *Surgery.* 2008;143:759–768.
28. van der Harst E, Bruining HA, Jaap Bonjer H, et al. Proliferative index in phaeochromocytomas: does it predict the occurrence of metastases? *J Pathol.* 2000;191:175–180.
29. Brown HM, Komorowski RA, Wilson SD, Demeure MJ, Zhu YR. Predicting metastasis of pheochromocytomas using DNA flow cytometry and immunohistochemical markers of cell proliferation: a positive correlation between MIB-1 staining and malignant tumor behavior. *Cancer.* 1999;86:1583–1589.
30. Martiniova L, Lu J, Chiang J, et al. Pharmacologic modulation of serine/threonine phosphorylation highly sensitizes PHEO in a MPC cell and mouse model to conventional chemotherapy. *PLoS One.* 2011;6:e14678.
31. Imperiale A, Moussallieh FM, Roche P, et al. Metabolome profiling by HRMAS NMR spectroscopy of pheochromocytomas and paragangliomas detects SDH deficiency: clinical and pathophysiological implications. *Neoplasia.* 2015;17:55–65.
32. Matro J, Giubellino A, Pacak K. Current and future therapeutic approaches for metastatic pheochromocytoma and paraganglioma: focus on SDHB tumors. *Horm Metab Res.* 2013;45:147–153.
33. Powers JF, Korgaonkar PG, Fliedner S, et al. Cytocidal activities of topoisomerase 1 inhibitors and 5-azacytidine against pheochromocytoma/paraganglioma cells in primary human tumor cultures and mouse cell lines. *PLoS One.* 2014;9:e87807.